Soft Matter

Cite this: *Soft Matter*, 2011, **7**, 10122

www.rsc.org/softmatter

PAPER

Examination of wettability and surface energy in fluorodecyl POSS/polymer blends†

Adam J. Meuler,[ab] Shreerang S. Chhatre,[a] Amarilys Rivera Nieves,[a] Joseph M. Mabry,[b] Robert E. Cohen*[a] and Gareth H. McKinley*[c]

Received 28th May 2011, Accepted 19th August 2011
DOI: 10.1039/c1sm05994g

Fluorodecyl Polyhedral Oligomeric SilSesquioxane (POSS) is a low surface energy material ($\gamma_{sv} \approx 10$ mN m^{-1}) that has been used as a coating to prepare a variety of liquid repellent surfaces. There are several drawbacks to employing pure fluorodecyl POSS as a coating, including high cost, poor adherence to the underlying substrate, and a lack of optical transparency. One potential strategy for overcoming these shortcomings while retaining liquid repellency is to prepare composite coatings by judiciously blending polymers with fluorodecyl POSS. Here varying amounts of fluorodecyl POSS are blended with commercially available poly(methyl methacrylate) (PMMA), poly(ethyl methacrylate) (PEMA), poly(butyl methacrylate) (PBMA), and the commercial fluoroelastomer Tecnoflon BR9151. A film of each blend is spin cast onto a silicon wafer and its surface wettability is probed by measuring advancing and receding contact angles of six liquids: water, ethylene glycol, dimethyl sulfoxide, diiodomethane, rapeseed oil, and hexadecane. Surface energy analysis techniques developed by Girifalco, Good, and colleagues are used to extract the hydrogen bond donating (acidic), hydrogen bond accepting (basic), and nonpolar (dispersion) components of the solid surface energy from both advancing and receding contact angle measurements. It is emphasized that a proper assessment of the wetting behavior of a liquid on a surface requires consideration of the complementary acid–base interactions between the solid and the liquid, not just a determination of the polar contribution to the solid surface energy. Maximum liquid repellency is attained in composite PMMA or PEMA films with fluorodecyl POSS loadings of at least 20 wt %. Furthermore, cross-cut adhesion tests reveal that the optically transparent methacrylate-containing fluorodecyl POSS coatings adhere quite strongly to the underlying substrate, unlike the Tecnoflon-containing blends and the pure fluorodecyl POSS. These results will potentially facilitate the incorporation of fluorodecyl POSS into commercial coatings.

Introduction

Surfaces that resist wetting by liquids are of interest for a wide variety of applications, including ink release surfaces for printers,[1] seals/gaskets,[2] and stain-resistant fabrics.[3–8] The wettability (or, conversely, repellency) of a substrate is sensitive to both topographical texture and surface chemistry,[9–11] the latter of which is the focus of this manuscript. A commonly employed strategy for reducing liquid wettability is to coat substrates with films of low surface energy materials. Zisman and colleagues established that the surface energy values of chemical groups decrease in the order $-CH_2- > -CH_3 > -CF_2- > -CF_3$,[12] and substantial research efforts have focused on the development of coatings that enhance liquid repellency by preferentially locating low energy moieties at or near the solid-air interface.[11,13–16]

One class of materials that has recently received attention as potential liquid repellent coatings is Polyhedral Oligomeric SilSesquioxanes (POSS). POSS compounds are thermally stable molecules comprised of silicon-oxygen cores with organic groups attached to the apex of each silicon atom, and they have found widespread application as additives to enhance the bulk properties of polymer-POSS nanocomposites.[17,18] Recent investigations have demonstrated that POSS materials also hold promise as surface modifiers. One particularly promising POSS compound, and the most liquid repellent of the POSS molecules

[a]*Department of Chemical Engineering, Massachusetts Institute of Technology, Cambridge, MA, USA. E-mail: recohen@mit.edu*
[b]*Air Force Research Laboratory, Edwards Air Force Base, CA, USA*
[c]*Department of Mechanical Engineering, Massachusetts Institute of Technology, Cambridge, MA, USA. E-mail: gareth@mit.edu*

† Electronic supplementary information (ESI) available: Surface tensions of the six probe fluids, advancing and receding liquid contact angles on all of the test surfaces, a plot of S_α as a function of $\bar{\theta}$, chemical structures of Tecnoflon, PMMA, PEMA, and PBMA, photographs of diiodomethane droplets advancing on a on 80/20 PBMA/fluorodecyl POSS sample, XPS survey and high resolution carbon 1s spectra for 80/20 PEMA/fluorodecyl POSS and 80/20 Tecnoflon/fluorodecyl POSS, and photographs of silicon wafers that were coated with 80/20 PEMA/fluorodecyl POSS or 80/20 Tecnoflon/fluorodecyl POSS and subjected to a cross-cut adhesion test. See DOI: 10.1039/c1sm05994g

described in the literature to date, is (1*H*,1*H*,2*H*,2*H*-heptadecafluorodecyl)$_8$Si$_8$O$_{12}$, or fluorodecyl POSS;[19–21] the structure of this molecule is provided in Fig. 1. Droplets of liquids with a range of surface tension values ($15.5 \leq \gamma_{lv} \leq 72.1$ mN m^{-1}) systematically form higher advancing and receding contact angles on flat films of fluorodecyl POSS than they do on coatings of alternative POSS species or on commercial fluoropolymers such as Tecnoflon or Teflon. The high liquid contact angles adopted by droplets on fluorodecyl POSS coatings are attributed to a synergistic combination of the rigid silicon-oxygen cage and the long fluorodecyl side chains.[21]

There is little consensus in the literature as to specific attributes that categorize a substrate as "liquid repellent," "hydrophobic," or "oleophobic." Often single static contact angles of probe liquids are used to provide some quantification of the wettability of a surface. Static contact angles generally fail to adequately describe the wetting behavior of liquid drops on surfaces, however, and characterizing wettability on the basis of such measurements is of limited utility.[22–24] A more useful characterization of wettability can be completed by considering the two physical processes by which sessile liquid drops can be removed from substrates. First, a surface can be tilted (or, alternatively, rotated rapidly[25]) to induce sliding or rolling of a sessile liquid drop. The angle of tilt required to induce drop motion (α) does not correlate with any single measured contact angle,[22,23,26–28] but can be predicted using measured receding and advancing contact angles θ_{rec} and θ_{adv} and an equation proposed by Furmidge:[29]

$$\sin(\alpha) = \frac{\gamma_{lv}}{mg} w(\cos\,\theta_{rec} - \cos\,\theta_{adv}) \quad (1)$$

where m is the mass of the drop, g is the gravitational constant, γ_{lv} is the liquid–vapor surface tension of the liquid, and w is the width of the drop perpendicular to the drop sliding direction. Eqn (1) is broadly consistent with experimental data,[25,29,30] though a truly rigorous quantitative prediction of the drop sliding angle requires consideration of the detailed shape of the contact line of a liquid droplet and the propensity for contact line pinning.[31,32] The sliding angle α clearly depends on the dimensionless contact angle hysteresis (CAH) in the form ($\cos\,\theta_{rec} - \cos\,\theta_{adv}$), not on a single contact angle value.[22,23] This hysteresis term is not, however, the only parameter in eqn (1) that is sensitive to the liquid contact angles; the drop width w also varies with liquid contact angles[27] and may be estimated using the expression:

$$w \approx 2\left(\frac{3V}{\pi}\right)^{1/3} \frac{\sin\bar{\theta}}{(2 - 3\cos\bar{\theta} + \cos^3\bar{\theta})^{1/3}} \quad (2)$$

where V is the drop volume and $\bar{\theta}$ is a cosine-averaged apparent contact angle that can be computed from the expression

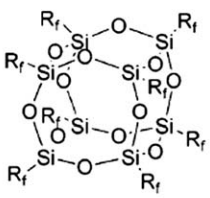

Fig. 1 Chemical structure of fluorodecyl POSS adapted from ref. 20.

$\cos\bar{\theta} = \frac{1}{2}(\cos\theta_{adv} + \cos\theta_{rec})$.[33] Defining density as $\rho = m/V$ and substituting the expression for w from eqn (2) into eqn (1) yields:

$$\sin(\alpha) \approx \frac{2\gamma_{lv}}{\rho g}\left(\frac{3}{\pi V^2}\right)^{1/3} \frac{\sin\bar{\theta}(\cos\theta_{rec} - \cos\theta_{adv})}{(2 - 3\cos\bar{\theta} + \cos^3\bar{\theta})^{1/3}} = \frac{2\gamma_{lv}}{\rho g}\left(\frac{3}{\pi V^2}\right)^{1/3} S_\alpha \quad (3)$$

where the drop sliding scaling factor S_α contains all of the terms that are functions of the liquid-surface interactions. This factor S_α is primarily sensitive to contact angle hysteresis in the form ($\cos\,\theta_{rec} - \cos\,\theta_{adv}$) but also contains some dependency on the absolute magnitudes of θ_{adv} and θ_{rec} due to the influence of $\bar{\theta}$ on the estimated drop width w. The sensitivity of the sliding angle α to the mean contact angle $\bar{\theta}$ reflects the fact that, all else equal, liquids characterized by higher magnitude contact angles will form narrower cross-section drops that slide more readily than the flatter sessile drops formed by liquids with smaller contact angles and larger contact areas. Quantitatively, these estimated $\bar{\theta}$-containing terms modify the hysteresis dependency ($\cos\,\theta_{rec} - \cos\,\theta_{adv}$) by a numerical factor that is generally between 3 ($\bar{\theta} \approx 3°$) and 0.1 ($\bar{\theta} \approx 170°$); a complete plot of this functional dependence as $\bar{\theta}$ varies is provided in Fig. S1 in the ESI.†

A second method to physically remove a sessile liquid drop is to pull the drop vertically off of a substrate. Such a process is often analyzed using thermodynamic work arguments to account for the individual free energy changes associated with the pairwise formation and elimination of specific interfaces. The Young-Dupré equation is commonly used to calculate the equilibrium work of adhesion (W_e) which is defined as the reversible free energy associated with the creation and destruction of interfaces:

$$W_e = \gamma_{lv}(1 + \cos\,\theta_e) \quad (4)$$

where θ_e is the equilibrium (Young's) contact angle.[11,34–37] There are several drawbacks to estimating the solid surface energy W_e using equilibrium (Young's) contact angle θ_e. Firstly, θ_e is difficult to measure[23,24,38,39] and, perhaps more importantly, θ_e and, by extension, γ_{sv} do not typically correlate well with the actual work required to remove liquid drops from substrates. For example, the forces required to remove Wilhelmy plates from liquids[11,37] or to separate surfaces connected by a capillary bridge of water[40] are dependent on the receding contact angle θ_{rec} and not the equilibrium contact angle θ_e. Gao and McCarthy suggested[22,23] that the practical work of adhesion[41] W_p that corresponds to the actual work required to separate a liquid from a surface could be calculated using a modified version of eqn (4) that replaces θ_e with the receding contact angle θ_{rec}:

$$W_p = \gamma_{lv}(1 + \cos\,\theta_{rec}) \quad (5)$$

The practical work required to remove a liquid drop from a surface is minimized when θ_{rec} is maximized, and is not related explicitly to the idealized value of the equilibrium contact angle θ_e.

An alternative approach to using measurements of θ_e to estimate γ_{sv} is to utilize measurements of the advancing and receding contact angles θ_{adv} and θ_{rec} to calculate an "advancing surface

energy" $\gamma_{sv,a}$ and a "receding surface energy" $\gamma_{sv,r}$ for a test sample.[21,24,42–44] Advantageously, measurements of both θ_{adv} and θ_{rec}, unlike those of θ_e, are readily reproducible[23–25,39] and, furthermore, are reliable predictors of the propensity for drop sliding described in eqn (3) or the ease of drop pull-off summarized in eqn (5). This advancing/receding surface energy approach is not derived from any fundamental theory, but can yield quantifiable and repeatable parameters that provide an empirical characterization of the liquid repellency (or, conversely, wettability) of a smooth substrate with a given surface chemistry.

Semiempirical models of solid surface energy that are commonly fit to contact angle data include those developed by Zisman,[12] Owens and Wendt,[45] and Girifalco, Good, and colleagues.[43,46–49] We use the version developed by Girifalco, Good, and coworkers to model the surface energy values of our test materials. Only a brief description of this framework is provided here, and more detailed treatments are available in the literature.[21,43,46–49]

According to the Girifalco-Good model, the total surface energy of either a solid (γ_{sv}) or a liquid (γ_{lv}) is the sum of the dispersion (or nonpolar, γ^d) and polar (γ^p) contributions. The polar portion can be further subdivided into hydrogen bond donating (or acidic, γ^+) and hydrogen bond accepting (or basic, γ^-) components:

$$\gamma_{lv} = \gamma_{lv}^d + \gamma_{lv}^p = \gamma_{lv}^d + 2\sqrt{\gamma_{lv}^+\gamma_{lv}^-}$$
$$\gamma_{sv} = \gamma_{sv}^d + \gamma_{sv}^p = \gamma_{sv}^d + 2\sqrt{\gamma_{sv}^+\gamma_{sv}^-} \quad (6)$$

The surface energy components of many probe liquids are known[50] based on water as a standard state with $\gamma_{lv}^+ = \gamma_{lv}^- = 25.5\ \mathrm{mN\ m^{-1}}$ and some of these values are provided in Table S1 in the ESI.† The expressions provided in eqn (6) can be combined with eqn (5) (either as written, or with θ_{adv} substituted for θ_{rec}) to yield expressions for the advancing and practical works of adhesion W_a and W_p:

$$W_a = \gamma_{lv}(1+\cos\theta_{adv}) = 2\left(\sqrt{\gamma_{sv,a}^d\gamma_{lv}^d} + \sqrt{\gamma_{sv,a}^+\gamma_{lv}^-} + \sqrt{\gamma_{lv}^+\gamma_{sv,a}^-}\right)$$
$$W_p = \gamma_{lv}(1+\cos\theta_{rec}) = 2\left(\sqrt{\gamma_{sv,r}^d\gamma_{lv}^d} + \sqrt{\gamma_{sv,r}^+\gamma_{lv}^-} + \sqrt{\gamma_{lv}^+\gamma_{sv,r}^-}\right) \quad (7)$$

Note that all of the energetic terms in these expressions are cross products between the solid and liquid parameters.[36] The unknown quantities $\gamma_{sv,i}^d$, $\gamma_{sv,i}^+$, and $\gamma_{sv,i}^-$ can be calculated from measurements of the advancing or receding contact angles of three contacting liquids and the following linear system of equations:

$$2\begin{bmatrix} \sqrt{\gamma_{lv,i,1}^d} & \sqrt{\gamma_{lv,i,1}^-} & \sqrt{\gamma_{lv,i,1}^+} \\ \sqrt{\gamma_{lv,i,2}^d} & \sqrt{\gamma_{lv,i,2}^-} & \sqrt{\gamma_{lv,i,2}^+} \\ \sqrt{\gamma_{lv,i,3}^d} & \sqrt{\gamma_{lv,i,3}^-} & \sqrt{\gamma_{lv,i,3}^+} \end{bmatrix}\begin{bmatrix} \sqrt{\gamma_{sv,i}^d} \\ \sqrt{\gamma_{sv,i}^+} \\ \sqrt{\gamma_{sv,i}^-} \end{bmatrix} = \begin{bmatrix} \gamma_{lv,i,1}(1+\cos\theta_{i,1}) \\ \gamma_{lv,i,2}(1+\cos\theta_{i,2}) \\ \gamma_{lv,i,3}(1+\cos\theta_{i,3}) \end{bmatrix} \quad (8)$$

This protocol was previously used to characterize spin-cast surfaces of fluorodecyl POSS, which has an advancing surface energy $\gamma_{sv,a} = 9.5 \pm 1.5\ \mathrm{mN\ m^{-1}}$ and a receding surface energy $\gamma_{sv,r} = 16.3 \pm 2.4$ mN/m.[21]

These low values of $\gamma_{sv,a}$ and $\gamma_{sv,r}$ indicate that fluorodecyl POSS interacts weakly with contacting liquids, and is a strongly "liquid repellent" material with respect to both the sliding and pull-off mechanisms summarized in eqn (3) and 5, respectively. Despite these unusually low surface energy values (particularly $\gamma_{sv,r}$), there are several drawbacks to employing pure fluorodecyl POSS as a liquid repellent coating. First, the morphology of films composed of crystalline POSS molecules is sensitive to the deposition conditions, with both smooth[21,51] and rough[8,20] coatings reported in the literature. For fully-wetted Wenzel state[9] droplets, increases in surface roughness generally lead to decreases in receding liquid contact angles and a concomitant increase in adhesion to the substrate,[11,30] a detrimental result if maximum liquid repellency is desired. Pure POSS films may also contain crystallites that are large enough to scatter light and reduce optical transparency, a drawback for numerous applications. Additionally, the weak intermolecular interactions that make fluorodecyl POSS coatings liquid repellent also reduce the adhesion of deposited fluorodecyl POSS films to underlying substrates, limiting their abrasion resistance and durability in coatings applications. Finally, POSS molecules are generally more expensive than alternative materials such as polymers, and minimizing the amount of fluorodecyl POSS that must be applied to a substrate to impart maximum liquid repellency is economically beneficial.

One strategy for addressing the shortcomings of pure POSS coatings is to use the POSS molecules as surface-modifying additives in blends with polymers. The POSS molecules in such blends locally phase separate from the polymeric chains and bloom to the composite/air interface in order to lower the system free energy, imparting the composite material with at least some of the liquid repellency characteristics of the POSS component.[51,52] Researchers pursuing this strategy have reported increases in liquid contact angles by adding various types of POSS molecules to polyurethanes,[52] nylon 6,[53] polycarbonate,[54] poly(methyl methacrylate),[7,51,55–60] poly(ethyl methacrylate),[4,61] polypropylene,[62] epoxy thermosets,[63] poly(chlorotrifluoroethylene),[64] fluoropolymer resin,[65] perfluorocyclobutyl aryl ether polymers,[2,66,67] and the commercial fluoroelastomer Tecnoflon BR9151.[5,61,68]

Here we investigate blends of fluorodecyl POSS with the fluoroelastomer Tecnoflon BR9151 and three polymethacrylates with a broad range of glass transition temperatures: poly(methyl methacrylate) (PMMA, $T_g = 124$ °C), poly(ethyl methacrylate) (PEMA, $T_g = 77$ °C), and poly(butyl methacrylate) (PBMA, $T_g = 18$ °C). These polymers are attractive candidates as the matrix component of polymer/fluorodecyl POSS composites because, unlike many alternative materials, they readily dissolve in the fluorinated solvent Asahiklin AK225 along with the fluorodecyl POSS. The molecular structures of these four polymers are provided in Fig. S2 in the ESI.† The advancing and receding contact angles of water, ethylene glycol, dimethyl sulfoxide, diiodomethane, rapeseed oil, and hexadecane are measured goniometrically on all of the test surfaces and these data are then used to evaluate advancing and receding surface energy values of polymer/fluorodecyl POSS blends within the context of the Girifalco-Good framework.[43,46,47] The lowest surface energy

values and maximum liquid repellencies are attained in PEMA or PMMA blends containing as little as 20 wt% fluorodecyl POSS. Furthermore, these composite coatings are readily deposited as smooth, optically transparent films that adhere strongly to underlying substrates.

Experimental

Materials

Asahiklin (AK225, Asahi Glass Company), ethylene glycol (99%, Aldrich), dimethyl sulfoxide (99%, Aldrich), diiodomethane (99%, Aldrich), rapeseed oil (Fluka), and hexadecane (99%, Aldrich) were used as received. Deionized water (18 MΩ-cm) was purified using a Millipore system. Tecnoflon BR9151 (Solvay Solexis), PMMA (Scientific Polymer Products, M_w = 540 kg mol^{-1}), PEMA (Aldrich, M_w = 515 kg mol^{-1}), PBMA (Aldrich, M_w = 337 kg mol^{-1}), Polycarbonate (PC, Bayer), 1*H*,1*H*,2*H*,2*H*-perfluorodecyltrichlorosilane (Aldrich), and Teflon AF-2400 solution (DuPont, item number 400S2-100-1) were used as received. We note that many different fluoropolymers are marketed under the "Teflon" name. The amorphous Teflon AF-2400 is characterized by higher θ_{adv} and θ_{rec} and thus lower $\gamma_{sv,a}$ and $\gamma_{sv,r}$ than most other Teflon materials,[22,69] making it a minimum surface energy benchmark for Teflon. Fluorodecyl POSS was prepared following established protocols.[20]

Differential scanning calorimetry (DSC)

Calorimetry experiments were conducted using a TA Instruments Q1000 DSC. Approximately 5 mg of each polymer was placed into an aluminum pan, heated at 10 °C min^{-1} to 180 °C, cooled at 10 °C min^{-1} to −80 °C, and heated again at 10 °C min^{-1} to 180 °C. Data were acquired during the second heating cycle.

Coating methodology

Polymer/fluorodecyl POSS solutions were prepared by dissolving polymers and/or fluorodecyl POSS in Asahiklin. Dichloromethane was used to prepare the PC solution because PC is not soluble in Ashahiklin. All of the polymer and polymer/fluorodecyl POSS solutions contained a total solids concentration of 20 mg/mL. Approximately 200–300 nm thick coatings of test materials were deposited at room temperature on silicon wafers *via* a spin coating process; about 0.5 mL of solution was placed on top of each silicon wafer (~4 cm^2) and the wafer was spun at 900 rpm for 30 s.

Amorphous Teflon AF-2400 was deposited onto a silicon wafer by: (i) placing ~0.5 mL of solution on top of a silicon wafer (~4 cm^2) and spinning the wafer at 900 rpm for 30 s; (ii) heating the film overnight at ~250 °C to evaporate the low-volatility fluorinated solvent.

Silicon wafers were treated with 1*H*,1*H*,2*H*,2*H*-perfluorodecyltrichlorosilane by: (i) placing them, along with a few drops of the reactive fluoroalkylsilane liquid, inside a Teflon canister under an inert nitrogen atmosphere; (ii) sealing the canister and heating it overnight at 150 °C.

Surface characterization

Scanning electron microscopy (SEM) images were acquired using a JEOL 6060 instrument operating at an acceleration voltage of 5 kV. Specimens were sputter coated with ~2 nm of platinum prior to imaging. Atomic force microscopy (AFM) measurements were carried out using a Dimension 3100 instrument (Veeco Metrology Group) operating in the tapping mode.

X-ray photoelectron spectroscopy (XPS) was performed using a Kratos Axis Ultra X-ray photoelectron spectrometer manufactured by Kratos Analytical (Manchester, England). The monochromatized Al Kα source was operated at 15 kV and 10 mA (150 W) and emissions were collected at takeoff vectors orthogonal to the sample surface.

Contact angle measurements

Contact angles of probe fluids on test surfaces were measured using a VCA2000 goniometer (AST Inc.). Advancing (θ_{adv}) and receding (θ_{rec}) angles were measured as probe fluid was supplied *via* a syringe into or out of sessile droplets (drop volume ~5 μL). Measurements were taken at four different spots on each film, and the reported uncertainties are standard deviations associated with these eight contact angle values (a left-side and right-side measurement for each drop).

Methodology for computing surface energy values

While in principle the matrix presented in eqn (8) is solvable using the advancing and receding contact angles of just three liquids, small uncertainties in the measured contact angles associated with the vector on the right hand side may yield large differences in the computed surface energy parameters when the system is mathematically ill-conditioned.[70,71] We reduce the impact of outlying data points and minimize the uncertainty by using the contact angle measurements from all six probe liquids on each of our test surfaces. Having six data points and just three unknowns yields an overdetermined set of equations that can be "solved" according to a least squares criterion. However, the three nonpolar liquids have only dispersion interactions (*i.e.*, $\gamma_{lv}^{+} = \gamma_{lv}^{-} = 0$), which makes the problem ill-conditioned. The matrix inversion process for this multicollinear system introduces significant uncertainty into the computed surface energy parameters if they are obtained from a simultaneous least squares fit of all of the experimental data.[72] Instead of considering simultaneously all of the data, an alternative two-step approach can be used:[73] (1) calculate the dispersion component of the solid surface energy $\gamma_{sv,i}^{d}$ from the measured nonpolar liquid contact angles; (2) determine least squares fits of $\gamma_{sv,i}^{+}$ and $\gamma_{sv,i}^{-}$ from this computed $\gamma_{sv,i}^{d}$ and the measured polar liquid contact angles. Such an approach advantageously circumvents the issues with multicollinearity error, incorporates information from all six liquids to minimize the impact of any one outlying data point, and ultimately yields meaningful values of $\gamma_{sv,i}^{d}$, $\gamma_{sv,i}^{+}$, and $\gamma_{sv,i}^{-}$.

Coating adhesion testing

The adhesion of deposited films to the underlying silicon wafers was probed by using a commercially available cross-cut test kit

(BYK Gardner, Cat. No. 5123) to follow an ASTM standard testing protocol.[74] Briefly, the supplier-provided flexible cutter was used to create a lattice pattern of cuts in each test film. These lattices consisted of eleven cuts, spaced 1 mm apart, that were made in two perpendicular directions. A piece of 25 mm wide semitransparent pressure sensitive tape (Permacel P99) was placed over the grid of cuts and rapidly peeled off of the surface at an angle of 180°. The coating was visually inspected and classified between 0B (worst adhesion) and 5B (best adhesion) according to ASTM standards.[74]

Results and discussion

The morphology and roughness of fluorodecyl POSS films prepared in this work varied in the same way as others previously described in the literature,[20,21,51] with both smooth and rough topographies resulting from the same deposition protocol of spin coating a 20 mg mL^{-1} solution at 900 rpm for 30 s. For example, one prepared "rough" fluorodecyl POSS film is characterized by water contact angles of $\theta_{adv} = 134°$ and $\theta_{rec} = 106°$ and a root-mean square roughness $R_q = 86$ nm while a "smooth" fluorodecyl POSS sample exhibits water contact angles of $\theta_{adv} = 125°$ and $\theta_{rec} = 112°$ and $R_q = 5.9$ nm. A scanning electron micrograph of the rough fluorodecyl POSS film is provided in Fig. 2a. We speculate that these variations can arise from interactions between the rate of solvent evaporation and the rate of fluorodecyl POSS crystallization as environmental variables such as temperature and relative humidity fluctuate. Blends comprising polymers and fluorodecyl POSS, in contrast, were consistently and reproducibly deposited as smooth films, and a representative scanning electron micrograph of an 80/20 PMMA/fluorodecyl POSS sample with water $\theta_{adv} = 124°$ and $\theta_{rec} = 118°$ and $R_q = 2.6$ nm is provided in Fig. 2b. Similarly smooth spin-coated films were obtained for all of the tested blends of fluorodecyl POSS and Tecnoflon, PMMA, PEMA, or PBMA. Promoting the deposition of smooth coatings is crucial for maximizing the receding contact angles of liquid drops and facilitating their removal from substrates by either the sliding (eqn (3)) or pull-off mechanism (eqn (5)) because receding contact angle, unlike advancing and most stable apparent contact angles,[38] decreases with roughness even when θ_{rec} measured on a smooth surface is above 90°.[11,30,75,76]

The smooth fluorodecyl POSS/polymer blends will exhibit maximum liquid repellency only if the chemical moieties located at or near the surface of the composite coating are those of the fluorodecyl POSS molecules, and not those of the higher energy

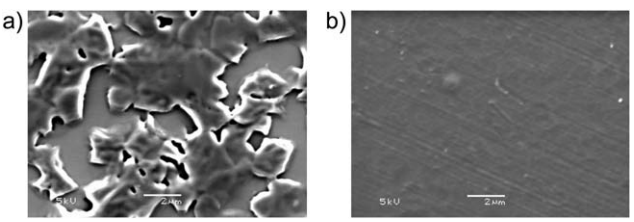

Fig. 2 Scanning electron micrographs of films of (a) "rough" fluorodecyl POSS and (b) 80/20 PMMA/fluorodecyl POSS spin cast onto silicon wafers. AFM analysis of 1 μm × 1 μm areas of the surfaces yielded root-mean square roughness R_q of (a) $R_q = 86$ nm (b) $R_q = 2.6$ nm.

polymers. Measurements of the advancing and receding contact angles of the bifunctional[36] polar (γ_{lv}^{+}, $\gamma_{lv}^{-} > 0$) liquids water, ethylene glycol, and dimethyl sulfoxide, as well as the nonpolar ($\gamma_{lv}^{-} = \gamma_{lv}^{+} = 0$) liquids diiodomethane, rapeseed oil, and hexadecane, provide a direct evaluation of the liquid wettability and an indirect probe of the surface composition of the polymer/fluorodecyl POSS blends. Representative data that illustrate key trends are presented in Fig. 3 and 4, and the complete set of advancing and receding contact angle measurements on the polymer/fluorodecyl POSS blends, polycarbonate, Teflon AF-2400,[77] and 1*H*,1*H*,2*H*,2*H*-perfluorodecyltrichlorosilane are provided in Tables S2 and S3 in the ESI.†

Water contact angle measurements for all of the tested polymer/fluorodecyl POSS materials are presented graphically in Fig. 3a. The advancing water contact angle increases rapidly as fluorodecyl POSS is added to each of the pure polymers, reaching $\theta_{adv} = 124 \pm 4°$ at fluorodecyl POSS loadings of 10 wt% and above ($f_{POSS} \geq 0.10$). The receding water contact angles also increase as fluorodecyl POSS is added to the polymers, but they plateau at different values for different polymeric binders. For PMMA, PEMA, and PBMA, θ_{rec} reaches 118 ± 2° for $f_{POSS} \geq 0.20$, while for the Tecnoflon-containing blends θ_{rec} increases more slowly as fluorodecyl POSS is added and only reaches 114 ± 1° when $f_{POSS} = 0.50$. Comparable maximum values in θ_{adv} and different plateaus in θ_{rec} are similarly obtained for the other polar probe fluids ethylene glycol and dimethyl sulfoxide on the test surfaces, as illustrated in Fig. 3b–3c. The data for the PEMA and PBMA materials essentially track those for the PMMA blends and are omitted from these plots to maximize clarity.

An alternative means of presenting these wettability data is to consider the sliding and pull-off mechanisms described by eqn (3) and 5, respectively. The two dimensionless solid-liquid interaction parameters that scale with the ease of drop removal by these processes are S_α for drop sliding (eqn (3)) and the quantity $(1 + \cos \theta_{rec})$ for drop pull-off (eqn (5)). A plot of S_α *versus* $(1 + \cos \theta_{rec})$ thus represents graphically the changes in the relative importance of these two physical processes. Data on this wettability plot must lie below and to the right of a curve that represents the limiting value $\theta_{adv} = 180°$ because it is not possible for θ_{rec} to exceed θ_{adv}. The resistance to drop sliding increases monotonically as S_α increases, with data points on the abscissa ($\theta_{adv} = \theta_{rec}$, $S_\alpha = 0$) indicative of drops that will slide or roll at any angle of tilt regardless of the magnitudes of θ_{adv} and θ_{rec}. The ease of drop sliding is not a complete description of liquid wettability, however, because it does not relate directly to the practical work of adhesion required to pull a liquid drop vertically off of a substrate.[22,23,27] This pull-off work scales with the parameter $(1 + \cos \theta_{rec})$ and increases monotonically with the distance along the abscissa. The most liquid-repellent substrates are characterized by both facile drop sliding (low ordinate value) and drop pull-off (low abscissa value), and are represented on this wettability diagram by the points nearest the origin.

The data for the bifunctional polar liquids water and dimethyl sulfoxide on Tecnoflon/fluorodecyl POSS blends and representative PMMA/fluorodecyl POSS materials are presented in this form in Fig. 3d. Ethylene glycol data for these surfaces substantially overlap with the corresponding dimethyl sulfoxide curves and are omitted from this diagram to maximize clarity.

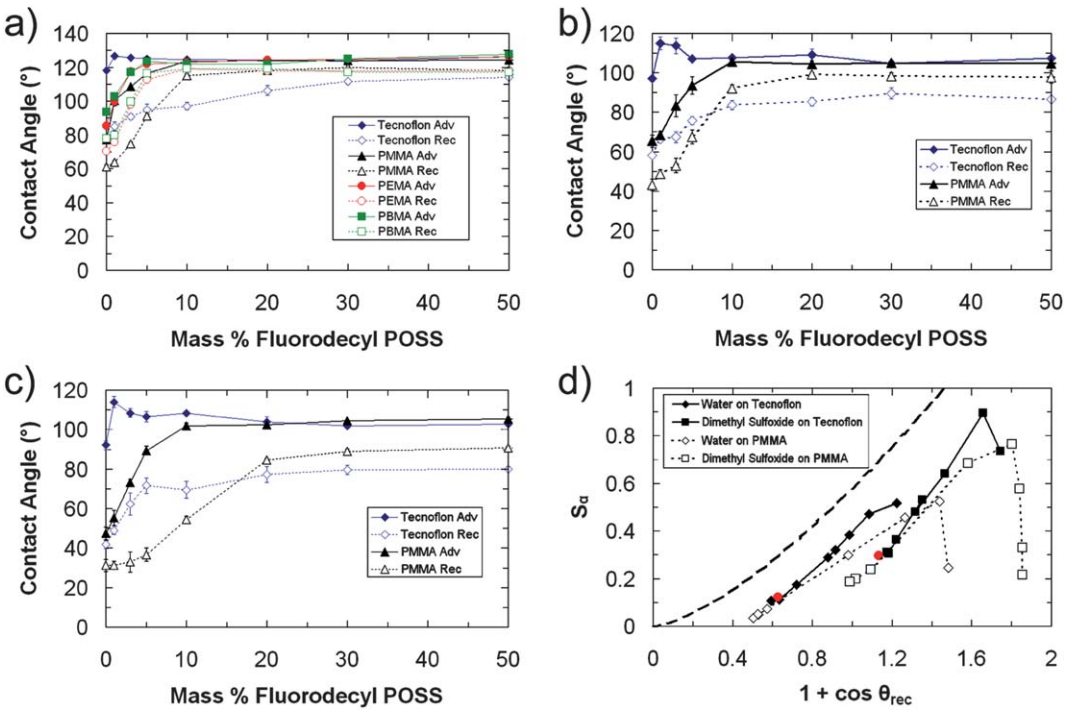

Fig. 3 The lines connecting the data points on all plots are intended to guide the eye. (a) Advancing and receding contact angles θ_{adv} and θ_{rec} for drops of water ($\gamma_{lv} = 72.1$ mN m^{-1}) on all of the tested polymer/fluorodecyl POSS surfaces. The solid symbols connote θ_{adv} and the hollow symbols denote θ_{rec}. (b) θ_{adv} and θ_{rec} for drops of ethylene glycol ($\gamma_{lv} = 47.7$ mN m^{-1}) on the PMMA/fluorodecyl POSS and Tecnoflon/fluorodecyl POSS materials. The solid symbols indicate θ_{adv} and the hollow symbols connote θ_{rec}. (c) θ_{adv} and θ_{rec} for drops of dimethyl sulfoxide ($\gamma_{lv} = 44.0$ mN m^{-1}) on the PMMA/fluorodecyl POSS and Tecnoflon/fluorodecyl POSS samples. The solid and hollow symbols denote θ_{adv} and θ_{rec}, respectively. (d) Liquid wettability diagram for water and dimethyl sulfoxide on the PMMA/fluorodecyl POSS and Tecnoflon/fluorodecyl POSS blends. The dimensionless wettability parameter (1 + cos θ_{rec}) for drop pull-off (eqn (5)) is plotted on the abscissa, while the term S_α that correlates with drop sliding (eqn (3)) is plotted on the ordinate. Points nearest the origin correspond to the most liquid-repellent substrates. The dashed line represents $\theta_{adv} = 180°$ and the area above and to the left of this curve is not accessible because it is impossible for $\theta_{rec} > \theta_{adv}$. The lines between data points connect the individual measurements, from right to left, in order of increasing fluorodecyl POSS loadings: 0 – 1 – 3 – 5 – 10 – 20 – 30 – 50 wt%. The red circles indicate measurements for the pure fluorodecyl POSS coating.

The curves for the polar liquid droplets on the PMMA blends get closer to the origin than those for the Tecnoflon materials, illustrating the enhanced repellency to such liquids for the polymethacrylate blends. The optimal polymethacrylate/fluorodecyl POSS samples are in fact more liquid repellent than a spin-cast pure fluorodecyl POSS film (red circles in Fig. 4d), likely due to the smoother surface topography, and consequent higher receding contact angles, of the polymer/fluorodecyl POSS blends, as discussed earlier.

A complete assessment of the liquid wettability of a substrate requires information about the behavior of both polar and nonpolar liquids that contact the surface. To probe the behavior of nonpolar liquids, advancing and receding contact angles of diiodomethane, rapeseed oil, and hexadecane were also measured on all of the test substrates. The advancing and receding contact angle values for diiodomethane on each of the polymer/fluorodecyl POSS test materials are plotted as a function of the fluorodecyl POSS loading in Fig. 4a. (Diiodomethane drops on the PBMA blends with $0.03 \leq f_{POSS} \leq 0.30$ advanced by a slip/stick process, as illustrated in Fig. S3 in the ESI,† and stable advancing contact angle values were not readily identified. Consequently, values of θ_{adv} for diiodomethane on these samples are not included in Fig. 4a.) Similar to the advancing contact angle data presented in Fig. 3, the diiodomethane advancing contact angles increase rapidly as fluorodecyl POSS is added to the pure polymers and reach an asymptotic limit of $\theta_{adv} = 104 \pm 3°$ for $f_{POSS} \geq 0.10$. The receding contact angles also increase with the addition of fluorodecyl POSS and level off at $\theta_{rec} = 88 \pm 4°$ when $f_{POSS} \geq 0.20$ for the PMMA, PEMA, and Tecnoflon blends. Receding contact angle measurements for diiodomethane drops on the PBMA materials, however, remain below this plateau, much like the polar liquid receding contact angle values did on the Tecnoflon blends in Fig. 3. In contrast to the dioodomethane behavior, the trends in receding contact angle for two other nonpolar liquids, rapeseed oil and hexadecane, are not substantially different for the PBMA-based materials and the other polymer/fluorodecyl POSS blends, as illustrated in Fig. 4b and 4c. The contact angle data for the Tecnoflon/fluorodecyl POSS and PEMA/fluorodecyl POSS materials follow the same trends as the PMMA/fluorodecyl POSS measurements and are omitted from these plots to maximize clarity.

Using the wettability diagram representation discussed earlier, the nonpolar liquid contact angle data for diiodomethane and hexadecane on the representative PMMA materials and outlying PBMA blends are replotted in Fig. 4d. The rapeseed oil data

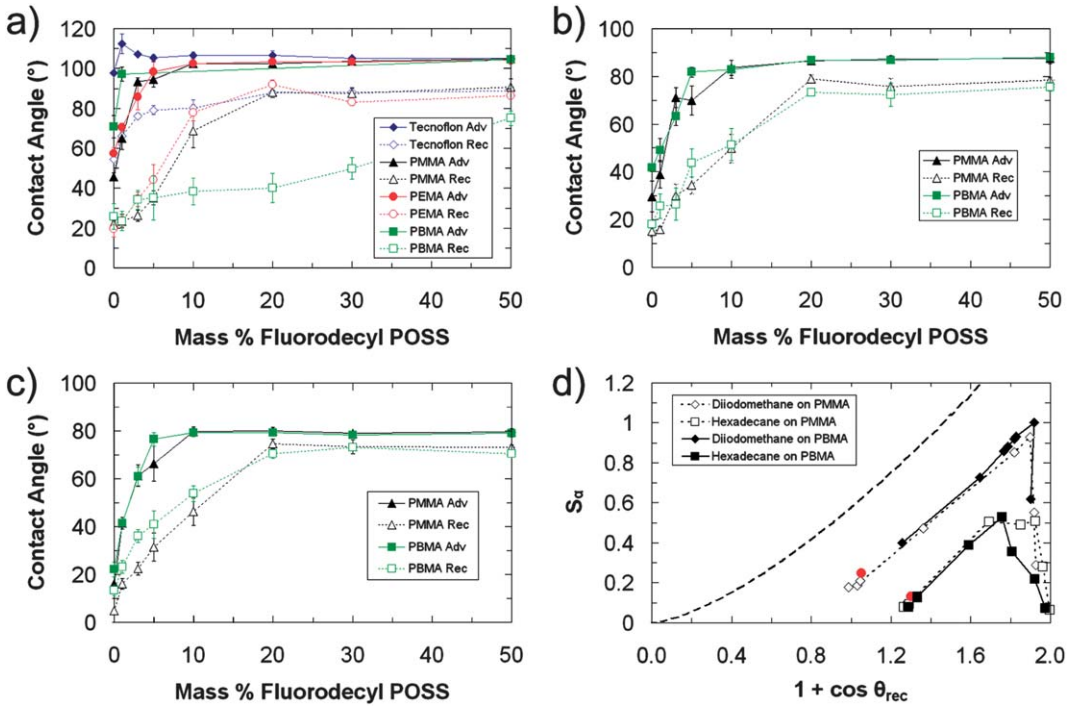

Fig. 4 The lines connecting the data points on all plots are meant to guide the eye. (a) Advancing and receding contact angles θ_{adv} and θ_{rec} for drops of diiodomethane (γ_{lv} = 50.8 mN m^{-1}) on all of the tested polymer/fluorodecyl POSS surfaces. The solid symbols denote θ_{adv} and the hollow symbols represent θ_{rec}. Diiodomethane drops advance by a slip/stick process on the PBMA-based materials with $0.03 \leq f_{POSS} \leq 0.30$, and stable values of θ_{adv} are difficult to ascertain and are thus not included on this plot for these selected samples (see Fig. S3 in the ESI).† (b) θ_{adv} and θ_{rec} for drops of rapeseed oil (γ_{lv} = 35.5 mN m^{-1}) on the PBMA/fluorodecyl POSS and PMMA/fluorodecyl POSS surfaces. The solid and hollow symbols represent θ_{adv} and θ_{rec}, respectively. (c) θ_{adv} and θ_{rec} for drops of hexadecane (γ_{lv} = 27.5 mN m^{-1}) on the PBMA/fluorodecyl POSS and PMMA/fluorodecyl POSS materials. The solid and hollow symbols connote θ_{adv} and θ_{rec}, respectively. (d) Nonpolar liquid wettability diagram for diiodomethane and hexadecane on the PMMA/fluorodecyl POSS and PBMA/fluorodecyl POSS blends. The dimensionless wettability parameter (1 + cos θ_{rec}) for drop pull-off (eqn (5)) is plotted on the abscissa, while the term S_α that correlates with drop sliding (eqn (3)) is plotted on the ordinate. Points nearest the origin correspond to the most liquid repellent substrates. The dashed line represents θ_{adv} = 180° and the area above and to the left of this curve is not accessible because it is impossible for θ_{rec} to exceed θ_{adv}. The lines between data points connect the individual measurements, from right to left, in order of increasing fluorodecyl POSS loadings: 0 – 1 – 3 – 5 – 10 – 20 – 30 – 50 wt%. The red circles represent measurements for the pure fluorodecyl POSS film. In this plot, the minimum observed advancing angle of 95° was assigned as θ_{adv} for diiodomethane drops on the PBMA blends with $0.03 \leq f_{POSS} \leq 0.30$. If any of the larger angles observed during diiodomethane drop advancing were used as θ_{adv}, S_α would be even higher, meaning our choice represents the maximum possible diiodomethane repellency for the PBMA materials.

overlap significantly with the hexadecane measurements and are excluded from this diagram to maximize clarity. The termination of the hexadecane (and omitted rapeseed oil) curves at essentially the same spot for both sets of materials illustrates that the maximum liquid repellency of these two liquids is similar on the PBMA-based and PMMA-based samples. In contrast, the curve for droplets of diiodomethane with γ_{lv} = 50.8 mN m^{-1} terminates closer to the origin for the PMMA materials than it does for the PBMA blends, illustrating that the diiodomethane repellency is higher for the optimal PMMA samples than for the best PBMA blend. As in Fig. 3, the optimal polymer/fluorodecyl POSS blends are even more liquid repellent than pure fluorodecyl POSS (red circles in Fig. 4d), most likely due to the increased roughness of the pure fluorodecyl POSS film.

The detailed shapes of the curves in Fig. 3d and 4d merit some discussion. The solid lines in the diagrams guide the eye by connecting the data points in the order of increasing fluorodecyl POSS content in the films. The wettability parameter (1 + cos θ_{rec}) decreases monotonically as the fluorodecyl POSS loading increases, with one exception: the pure fluorodecyl POSS films exhibit higher (1 + cos θ_{rec}) values than the PMMA blends with fluorodecyl POSS loadings of 20 wt% and above. We believe this slight decrease in θ_{rec} for the pure fluorodecyl POSS coatings is caused by subtle surface roughness effects in the pure films. In contrast to the quantity (1 + cos θ_{rec}), the sliding parameter S_α is not monotonic; it initially increases at low fluorodecyl POSS loadings, peaks, and then decreases towards an asymptotic minimum value. The initial rise in S_α is driven by an increase in contact angle hysteresis that results from θ_{adv} increasing more rapidly than θ_{rec} as fluorodecyl POSS is added to the neat polymers. The subsequent decrease in S_α occurs as θ_{adv} reaches a plateau while θ_{rec} continues to increase towards its asymptotic maximum value, which minimizes the hysteresis. The unequal rates of change in θ_{adv} and θ_{rec} are likely driven by different sensitivities of contact line pinning to the multiple components of a chemically heterogeneous surface. The advancing contact line is most sensitive to the low energy portion of the surface and increases rapidly as fluorodecyl POSS begins to occupy a significant fraction of the surface. The receding contact line, in contrast, is most sensitive to the high energy components of the

surface (*i.e.*, the polymer rich domains), and does not increase substantially until the fluorodecyl POSS domains cover nearly all of the surface.[11,24,43,70]

In general, pinning of the receding contact line and contact angle hysteresis are sensitive to three surface properties: roughness, chemical heterogeneity, and molecular rearrangements in the solid subphase.[11,78] Systematic differences in one or more of these surface attributes are likely responsible for the sensitivity of receding contact angle measurements for diiodomethane and polar liquid drops to the identity of the polymeric binder for the materials with $f_{POSS} \geq 0.20$. The contact angle data do not vary systematically with variations in roughness for the different polymeric binders, as only the polar liquids and diiodomethane exhibit a dependence of θ_{rec} on the identity of the polymer. The variations in liquid wettability for the different blend series must therefore be driven by specific interactions between certain contacting liquids and the blend surfaces. XPS was deployed to examine possible differences in chemical heterogeneity by probing the chemical composition of the top 10 nm[79,80] of films of 80/20 Tecnoflon/fluorodecyl POSS and 80/20 PEMA/fluorodecyl POSS. These XPS survey and high resolution carbon 1s spectra are provided in Fig. S4 in the ESI.† The atomic ratios calculated from these raw data are provided in Table 1 along with those expected for pure fluorodecyl POSS.[4] The values for the two test surfaces are essentially identical, and very close to those expected for pure fluorodecyl POSS. These results are consistent with the fluorodecyl POSS molecules blooming up and minimizing chemical heterogeneity by covering nearly the entire surface of each blend.

Surface compositions can, however, be altered by molecular rearrangements that are induced by contact with the probe fluid.[11,78] Such reorientations lower the total free energy of the three phase system by increasing favorable interactions between the liquid and the underlying substrate and consequently reducing θ_{rec}.[78] We speculate that surface rearrangments are responsible for the systematically lower receding contact angle values measured for polar liquids on Tecnoflon/fluorodecyl POSS blends and for diiodomethane drops on PBMA/fluorodecyl POSS materials. Both Tecnoflon and PBMA contain segments that are rubbery and mobile at room temperature, as evidenced by the measured glass transition temperatures of −9 °C for Tecnoflon and 18 °C for PBMA. We posit that the acidic $–CF_2–CH_2–$ protons[69] in Tecnoflon and the dispersive alkyl segments in PBMA reorient to enhance favorable interactions with the appropriate contacting liquids. The glassy PMMA (T_g = 124 °C) and PEMA (T_g = 77 °C) segments do not, in contrast, possess sufficient mobility at room temperature to quickly reorient.

Table 1 Measured atomic ratios at the surfaces of 80/20 Tecnoflon/fluorodecyl POSS and 80/20 PEMA/fluorodecyl POSS materials and calculated atomic ratios for pure fluorodecyl POSS

Sample	F/C	O/C	Si/C
80/20 Tecnoflon/Fluorodecyl POSS	1.52[a]	0.11[a]	0.08[a]
80/20 PEMA/Fluorodecyl POSS	1.54[a]	0.11[a]	0.09[a]
Fluorodecyl POSS	1.7[b]	0.15[b]	0.1[b]

[a] Determined using XPS survey spectra. [b] Calculated values.[4]

The advancing and receding contact angle measurements for all six test liquids can be used in conjunction with the matrix formulation provided in eqn (8) and the protocol described in the Experimental Section to calculate the dispersion ($\gamma^d_{sv,i}$), acidic ($\gamma^+_{sv,i}$), and basic ($\gamma^-_{sv,i}$) components of the advancing and receding solid surface energy values $\gamma_{sv,a}$ and $\gamma_{sv,r}$. Advancing contact angle data for diiodomethane on the PBMA blends with $0.03 \leq f_{POSS} \leq 0.30$ are not used in these calculations because the drops advanced by a slip/stick mechanism, making the measurements unreliable for surface energy analysis.[81] The surface energy values for all of our test materials are provided in Table 2. Notably the fluorodecyl POSS materials are distinguishable from fluorinated alternatives such as Teflon AF-2400[77] and 1*H*,1*H*,2*H*,2*H*-perfluorodecyltrichlorosilane (fluoroalkylsilane), which is widely used[6,51] by the surface science community to reduce the liquid wettability of substrates. The key differences amongst these fluorinated materials do not appear in the often-considered advancing surface energy values $\gamma_{sv,a}$, which are comparable. Rather it is the receding surface energy values $\gamma_{sv,r}$ that are noticeably higher for Teflon AF-2400 and the fluoroalkylsilane than they are for the optimized fluorodecyl POSS-containing samples. It is the low receding surface energy values that minimize the resistance to both drop sliding and drop pull-off and distinguish fluorodecyl POSS as a strongly liquid repellent material.

Surface energy terms for selected representative test samples are plotted in Fig. 5 to examine the trends when fluorodecyl POSS is blended with the various polymers. In Fig. 5a we show the variation in the overall advancing and receding surface energy values $\gamma_{sv,a}$ and $\gamma_{sv,r}$ for the PMMA/fluorodecyl POSS and PBMA/fluorodecyl POSS blends as a function of the fluorodecyl POSS loading. The advancing surface energy values for both sets of materials decrease sharply as fluorodecyl POSS is blended with the pure polymers and reach a minimum value of $\gamma_{sv} \approx 9 \pm 1$ mN m^{-1} for fluorodecyl POSS loadings of 10 wt% and above. The calculated receding surface energy values of these two series of blends differ significantly, however, due to the marked differences in receding contact angles of diiodomethane drops. For the PMMA materials, $\gamma_{sv,r}$ declines as fluorodecyl POSS is added and reaches a minimum of $\gamma_{sv,r} = 13 \pm 1$ mN m^{-1} for $f_{POSS} \geq 0.20$. The receding surface energy values for the PBMA materials also decrease as fluorodecyl POSS is added, but do so to much less of an extent than they do for the PMMA blends and only reach a minimum value of 16 mN m^{-1} for $f_{POSS} = 0.50$. These elevated values of $\gamma_{sv,r}$ for PBMA surfaces are the result of larger dispersion interactions $\gamma^d_{sv,r}$. We speculate this increase in $\gamma^d_{sv,r}$ is driven by molecular rearrangements in the leathery PBMA materials ($T_g = 18$ °C) that are not prevalent in the glassy PMMA ($T_g = 124$ °C) and PEMA ($T_g = 77$ °C) chains.

The advancing and receding surface energy values of PMMA/fluorodecyl POSS and Tecnoflon/fluorodecyl POSS materials are plotted as a function of the fluorodecyl POSS loading in Fig. 5b. For both sets of materials, $\gamma_{sv,a}$ and $\gamma_{sv,r}$ decrease as the fluorodecyl POSS loadings are increased and reach plateaus of $\gamma_{sv,a} = 8 \pm 2$ mN for $f_{POSS} \geq 0.10$ and $\gamma_{sv,r} = 13 \pm 2$ mN for $f_{POSS} \geq 0.20$. Despite the statistically indistinguishable values of $\gamma_{sv,r}$ for samples with $f_{POSS} \geq 0.20$, the receding contact angles of polar liquids are consistently lower on the Tecnoflon materials than on the PMMA blends, as was shown in Fig. 3.

Table 2 Values of total ($\gamma_{sv,i}$), dispersion ($\gamma^d_{sv,i}$), polar ($\gamma^p_{sv,i}$), hydrogen bond donating ($\gamma^+_{sv,i}$), and hydrogen bond accepting ($\gamma^-_{sv,i}$) surface energy values calculated from advancing and receding contact angles[a]

Sample	Surface energy values from advancing contact angles (mN m^{-1})					Surface energy values from receding contact angles (mN m^{-1})				
	$\gamma_{sv,a}$	$\gamma^d_{sv,a}$	$\gamma^p_{sv,a}$	$\gamma^+_{sv,a}$	$\gamma^-_{sv,a}$	$\gamma_{sv,r}$	$\gamma^d_{sv,r}$	$\gamma^p_{sv,r}$	$\gamma^+_{sv,r}$	$\gamma^-_{sv,r}$
Teflon AF-2400	9.6	9.6	0.01	0.01	0.03	16.6	16.1	0.42	0.05[d]	0.82
Fluoroalkylsilane[b]	8.6	8.5	0.10	0.01[d]	0.53	22.7	21.2	1.5	0.11	5.1
PC	39.3	35.2	4.1	0.23[d]	18.4	40.4	38.3	2.1	0.10	11.4
PMMA	33.1	32.3	0.88	0.01[d]	13.3	39.6	37.9	1.7	0.03	23.1
99/1 PMMA/Fluorodecyl POSS	26.1	25.3	0.81	0.51	0.33	38.4	37.4	0.97	0.01	21.2
97/3 PMMA/Fluorodecyl POSS	14.5	13.4	1.1	0.95	0.30	37.7	35.6	2.1	0.10	10.7
95/5 PMMA/Fluorodecyl POSS	13.2	13.0	0.21	0.05	0.22	34.1	33.2	0.91	0.11	1.9
90/10 PMMA/Fluorodecyl POSS	9.2	9.2	0.04	0.01[d]	0.25	23.3	22.7	0.53	0.14	0.50[d]
80/20 PMMA/Fluorodecyl POSS	8.9	8.9	0.04	0.00	0.19	12.7	12.6	0.14	0.06	0.08
70/30 PMMA/Fluorodecyl POSS	8.7	8.7	0.01	0.00	0.26	13.3	13.2	0.03	0.01	0.04
50/50 PMMA/Fluorodecyl POSS	8.5	8.5	0.00	0.00	0.26	12.4	12.3	0.12	0.02	0.20
PEMA	29.7	28.6	1.1	0.04	7.0	38.6	38.1	0.53	0.01[d]	15.9
99/1 PEMA/Fluorodecyl POSS	22.9	21.8	1.1	0.18	1.7	37.3	36.4	0.94	0.02	10.6
97/3 PEMA/Fluorodecyl POSS	12.9	12.8	0.14	0.02	0.27	32.9	32.5	0.44	0.15	0.33
95/5 PEMA/Fluorodecyl POSS	10.0	9.9	0.07	0.01[d]	0.33	27.5	27.2	0.28	0.06	0.33[d]
90/10 PEMA/Fluorodecyl POSS	9.1	9.0	0.12	0.01[d]	0.38	15.9	15.8	0.09	0.06	0.04[d]
80/20 PEMA/Fluorodecyl POSS	8.9	8.9	0.02	0.00	0.16	12.3	12.1	0.21	0.03	0.32
70/30 PEMA/Fluorodecyl POSS	8.9	8.9	0.04	0.01	0.11	13.9	13.9	0.03	0.00	0.15
50/50 PEMA/Fluorodecyl POSS	8.6	8.6	0.03	0.01[d]	0.10	13.7	13.6	0.02	0.00	0.24
PBMA	25.4	25.3	0.12	0.00	4.7	41.2	37.0	4.3	0.33[d]	14.0
99/1 PBMA/Fluorodecyl POSS[c]	18.8	17.3	1.5	0.59	1.0	41.2	37.0	4.3	0.39[d]	12.2
97/3 PBMA/Fluorodecyl POSS[c]	17.7	17.0	0.70	0.27[d]	0.46	37.2	33.8	3.4	1.0[d]	2.8
95/5 PBMA/Fluorodecyl POSS[c]	11.2	11.1	0.16	0.04[d]	0.17	31.5	31.4	0.12	1.1[d]	0.01[d]
90/10 PBMA/Fluorodecyl POSS[c]	10.9	10.5	0.39	0.07[d]	0.52	29.0	28.7	0.32	0.99[d]	0.03[d]
80/20 PBMA/Fluorodecyl POSS[c]	10.2	9.8	0.38	0.06[d]	0.59	23.6	23.5	0.10	0.40[d]	0.01[d]
70/30 PBMA/Fluorodecyl POSS[c]	10.3	10.2	0.13	0.03[d]	0.13	22.4	21.6	0.83	0.68[d]	0.25
50/50 PBMA/Fluorodecyl POSS	8.5	8.5	0.01	0.00	0.01	16.1	16.0	0.10	0.02[d]	0.15
Tecnoflon	11.6	11.4	0.22	0.05	0.23	32.1	28.0	4.1	0.39	10.8
99/1 Tecnoflon/Fluorodecyl POSS	6.5	6.1	0.42	0.06[d]	0.78	25.4	19.8	5.6	1.2	6.6
97/3 Tecnoflon/Fluorodecyl POSS	7.3	7.0	0.27	0.03[d]	0.57	21.7	16.6	5.1	1.3	4.8
95/5 Tecnoflon/Fluorodecyl POSS	8.1	8.0	0.06	0.01[d]	0.30	18.6	15.1	3.5	0.65	4.9
90/10 Tecnoflon/Fluorodecyl POSS	8.0	7.9	0.14	0.01[d]	0.45	17.4	14.7	2.7	0.44	4.3
80/20 Tecnoflon/Fluorodecyl POSS	7.8	7.8	0.01	0.00	0.36	14.5	12.8	1.7	0.60	1.2
70/30 Tecnoflon/Fluorodecyl POSS	8.5	8.4	0.11	0.02	0.19	13.6	12.8	0.79	0.41	0.38
50/50 Tecnoflon/Fluorodecyl POSS	8.2	8.1	0.04	0.01	0.06	13.6	13.4	0.25	0.55	0.03
Fluorodecyl POSS	8.0	7.9	0.02	0.00	0.18	14.5	13.9	0.60	0.23	0.38

[a] Consideration of a typical error in contact angle measurement ($\Delta\theta \approx 2°$) and the condition number of the transformation matrix in the system of linear equations yields an approximately 15% relative error in the calculated surface energy values. [b] 1*H*,1*H*,2*H*,2*H*-Perfluorodecyltrichlorosilane. [c] Advancing contact angles of diiodomethane drops on PBMA blends with $0.01 \leq f_{POSS} \leq 0.30$ were difficult to measure (see Fig. S3 in the ESI) and were not used to calculate the advancing surface energy terms for these materials. [d] The square root of the computed surface energy parameter is a negative value.

Understanding the energetic characteristics that drive this difference in polar liquid wettability requires a closer examination of the subcomponents of $\gamma_{sv,r}$.

The polar contributions to the receding surface energy $\gamma^p_{sv,r}$ are plotted as a function of fluorodecyl POSS content for the PMMA-based and Tecnoflon-based materials in Fig. 5c. In contrast to the calculated values shown in Fig. 5b, here there is a clear difference between these two data sets, with the polar contribution $\gamma^p_{sv,r}$ always lower for the PMMA surfaces than for the Tecnoflon substrates. Such a result is consistent with the lower receding contact angles that were measured for droplets of polar liquids on the Tecnoflon-containing materials as compared to the PMMA samples (see Fig. 3 or Table S3 in the ESI†). However, the monotonic decrease in $\gamma^p_{sv,r}$ for the Tecnoflon/fluorodecyl POSS samples with increasing fluorodecyl POSS content does not correlate with the measured values of receding contact angles for ethylene glycol and dimethyl sulfoxide drops. Neither of these liquids exhibit values of θ_{rec} that increase as $\gamma^p_{sv,r}$ decreases. Rather, both fluids establish statistically indistinguishable values of the receding contact angle θ_{rec} on all of the Tecnoflon-based samples with at least 20 wt% fluorodecyl POSS.

The polar contribution to the receding surface energy $\gamma^p_{sv,r}$ does not correlate with the measured values of the receding contact angles for ethylene glycol and dimethyl sulfoxide because $\gamma^p_{sv,r}$ is a function of the product of the acidic and basic contributions to the solid surface energy $\gamma^+_{sv,r}$ and $\gamma^-_{sv,r}$, respectively, as defined in eqn (6). Liquid contact angles are not, however, sensitive to this product of solid surface parameters, but rather depend on the complementary acid/base interactions between the solid and the contacting fluid, as demonstrated in eqn (7).[36] Thus it is the cross products $\sqrt{\gamma^+_{sv,r}\,\gamma^-_{lv}}$ and $\sqrt{\gamma^-_{sv,r}\,\gamma^+_{lv}}$, and not $\gamma^p_{sv,r}$, that influence receding liquid contact angles. For our analysis, we selected the widely used,[50] albeit arbitrary,[43,70] reference state in which water

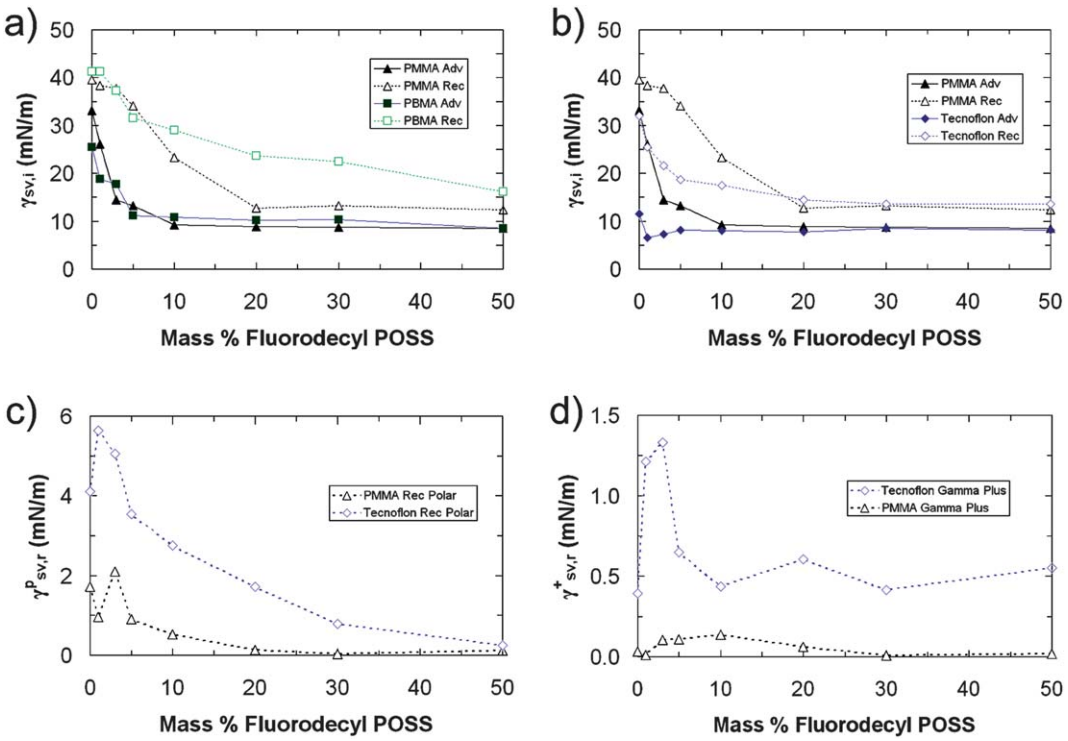

Fig. 5 Receding and advancing solid surface energy terms as the fluorodecyl POSS content of the blends is increased. Solid symbols denote advancing values while hollow symbols indicate receding terms. (a) Overall advancing and receding surface energy terms $\gamma_{sv,a}$ and $\gamma_{sv,r}$ for the PMMA/fluorodecyl POSS and PBMA/fluorodecyl POSS blends. (b) $\gamma_{sv,a}$ and $\gamma_{sv,r}$ for the PMMA/fluorodecyl POSS and Tecnoflon/fluorodecyl POSS materials. (c) Polar contributions to receding surface energy $\gamma^{p}_{sv,r}$ for the PMMA-based and Tecnoflon-based samples. (d) $\gamma^{+}_{sv,r}$ for the PMMA/fluorodecyl POSS and Tecnoflon/fluorodecyl POSS surfaces.

is characterized by equivalent acidic and basic components such that $\gamma^{+}_{lv} = \gamma^{-}_{lv} = 25.5$ mN/m. Most polar liquids other than water, including the ethylene glycol and dimethyl sulfoxide used in this work, are characterized as basic (*i.e.*, high values of γ^{-}_{lv}) when this reference state is used. The wettability of these more basic liquids is sensitive to the complementary acidic component of the solid surface energy $\gamma^{+}_{sv,r}$, and the magnitude of such contributions can be examined by computing the components of the practical work of adhesion (eqn (7)). These values are provided in Table 3 for the representative interactions between ethylene glycol and four different test surfaces, along with the measured values of the receding contact angle θ_{rec} for ethylene glycol. The substantial difference in the interactions between ethylene glycol (and other basic liquids) and these two sets of surfaces is that the $\sqrt{\gamma^{+}_{sv,r}\gamma^{-}_{lv}}$ contribution is significantly higher for the Tecnoflon blends than it is for the PMMA materials. The solid surface characteristic that influences this $\sqrt{\gamma^{+}_{sv,r}\gamma^{-}_{lv}}$ interaction is the term $\gamma^{+}_{sv,r}$, and this latter parameter is plotted as a function of fluorodecyl POSS loading for the PMMA and Tecnoflon materials in Fig. 5d. The $\gamma^{+}_{sv,r}$ values reach a plateau for both sample sets once the fluorodecyl POSS loading reaches 20 wt%, with the Tecnoflon $\gamma^{+}_{sv,r}$ plateau well above its PMMA counterpart.

We believe these differences in the acidic component of the solid surface energy $\gamma^{+}_{sv,r}$ reduce receding contact angles for basic liquids on Tecnoflon/fluorodecyl POSS samples with $f_{POSS} \geq 0.20$ below the values exhibited by the same fluids on PMMA blends with comparable fluorodecyl POSS loadings. Furthermore, the invariance in both $\gamma^{+}_{sv,r}$ and $\gamma^{d}_{sv,r}$ for $f_{POSS} \geq 0.20$ is consistent with the plateaus in polar liquid θ_{rec} that are reported in Table S3. This consistency with all aspects of the experimental

Table 3 Ethylene glycol receding contact angles and values of the contributions to the practical work of adhesion W_p for ethylene glycol on 80/20 PMMA/fluorodecyl POSS, 50/50 PMMA/fluorodecyl POSS, 80/20 Tecnoflon/fluorodecyl POSS, and 50/50 Tecnoflon/fluorodecyl POSS

		Absolute magnitudes (mN m^{-1})			Fraction of W_p		
Sample	Ethylene glycol θ^{rec}	$\sqrt{\gamma^{d}_{sv,r}\gamma^{d}_{lv}}$	$\sqrt{\gamma^{+}_{sv,r}\gamma^{-}_{lv}}$	$\sqrt{\gamma^{-}_{sv,r}\gamma^{+}_{lv}}$	$\sqrt{\gamma^{d}_{sv,r}\gamma^{d}_{lv}}$	$\sqrt{\gamma^{+}_{sv,r}\gamma^{-}_{lv}}$	$\sqrt{\gamma^{-}_{sv,r}\gamma^{+}_{lv}}$
80/20 PMMA/Fluorodecyl POSS	99.2 ± 0.8	19.0	1.7	0.1	0.91	0.08	0.01
50/50 PMMA/Fluorodecyl POSS	97.8 ± 3.1	18.8	0.9	0.6	0.92	0.05	0.03
80/20 Tecnoflon/Fluorodecyl POSS	85.5 ± 2.1	19.1	5.3	1.5	0.74	0.21	0.05
50/50 Tecnoflon/Fluorodecyl POSS	86.5 ± 1.6	19.6	5.1	0.2	0.79	0.20	0.01

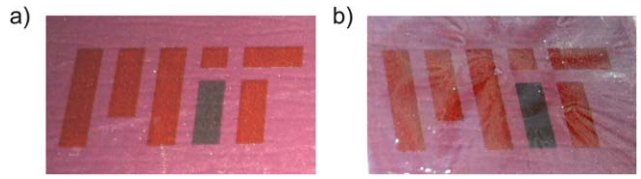

Fig. 6 Photographs of microscope slides placed over a fuchsia background. The slides were spin-coated with (a) 80/20 PEMA/fluorodecyl POSS and (b) fluorodecyl POSS. The coating in (a) is optically transparent and clear while white fluorodecyl POSS powder is visible in (b).

liquid contact angle trends makes $\gamma^{+}_{sv,r}$ (or $\gamma^{-}_{sv,r}$ for acidic liquids) a more relevant parameter than $\gamma^{p}_{sv,r}$ in the assessment of the liquid wettability of a surface. In general, consideration of the total polar contribution to the solid surface energy $\gamma^{p}_{sv,r}$ is of limited utility for several reasons.[36] First, $\gamma^{p}_{sv,r} = \sqrt{\gamma^{+}_{sv,r}\gamma^{-}_{sv,r}}$ is the product of the individual acidic and basic energetic characteristics of the solid surface itself. The solid surface is not interacting with itself, however, but rather with contacting liquids, and it is the cross products $\sqrt{\gamma^{+}_{sv,r}\gamma^{-}_{lv}}$ and $\sqrt{\gamma^{-}_{sv,r}\gamma^{+}_{lv}}$ that influence liquid wettability. Second, the polar contribution to the surface energy $\gamma^{p}_{sv,r}$ can have a small magnitude that makes it appear negligible relative to $\gamma^{d}_{sv,r}$ when either $\gamma^{+}_{sv,r}$ or $\gamma^{-}_{sv,r}$ is near zero. This apparently low contribution of polar terms can lead to the erroneous conclusion that polar liquids do not interact specifically with a surface. For example, the 50/50 Tecnoflon/fluorodecyl POSS and 50/50 PEMA/fluorodecyl POSS samples are characterized by comparable values of the total receding surface energy $\gamma_{sv,r}$, and for both materials the polar contributions $\gamma^{p}_{sv,r}$ are less than 2% of $\gamma_{sv,r}$. However, these similarities in $\gamma_{sv,r}$ and $\gamma^{p}_{sv,r}$ do not lead to comparable repellency for basic liquids. The receding contact angles of both dimethyl sulfoxide and ethylene glycol are higher on 50/50 PEMA/fluorodecyl POSS than they are on 50/50 Tecnoflon/fluorodecyl POSS. These differences in θ_{rec} can only be rationalized when $\gamma^{+}_{sv,r}$ (or $\gamma^{-}_{sv,r}$ for acidic liquids), $\gamma^{d}_{sv,r}$ and, by extension, the three subcomponents of the practical work of adhesion ($\sqrt{\gamma^{d}_{sv,r}\gamma^{d}_{lv}}$, $\sqrt{\gamma^{+}_{sv,r}\gamma^{-}_{lv}}$, and $\sqrt{\gamma^{-}_{sv,r}\gamma^{+}_{lv}}$) are evaluated.

The discussion to this point has established that the most liquid-repellent fluorodecyl POSS-containing materials studied here are the PMMA/fluorodecyl POSS and PEMA/fluorodecyl POSS blends with fluorodecyl POSS loadings of 20 wt% and above. These blends are generally even more liquid repellent than pure fluorodecyl POSS coatings because the addition of a polymeric binder facilitates the deposition of smooth films that minimize contact line pinning and liquid adhesion. There are numerous other benefits to mixing polymers with fluorodecyl POSS besides reducing coating roughness. First, as a result of surface segregation, only ~20 wt% fluorodecyl POSS is required to maximize liquid repellency. The PMMA and PEMA matrix polymers are significantly cheaper than the fluorodecyl POSS and widely available commercially, reducing the cost of liquid repellent fluorodecyl POSS-based coatings. Furthermore, the polymer/fluorodecyl POSS blends are optically transparent, as illustrated in Fig. 6a. Pure fluorodecyl POSS coatings, on the other hand, are hazy white powders that hinder transmission of visible light, as illustrated in Fig. 6b. Finally, cross-cut tape adhesion tests reveal that the PMMA/fluorodecyl POSS and PEMA/fluorodecyl POSS blends adhere significantly more strongly to the underlying substrates than either the Tecnoflon/fluorodecyl POSS or pure fluorodecyl POSS coatings. Large sections of an 80/20 Tecnoflon/fluorodecyl POSS blend (ASTM-categorized adhesion strength of 1B) and pure fluorodecyl POSS coating (3B) are removed from coated silicon wafers during the test while an 80/20 PEMA/fluorodecyl POSS film remains adhered to the underlying substrate (5B). Photographs of silicon wafers coated with the 80/20 blends and subjected to the cross-cut adhesion test are provided in the ESI.† The high surface energy of the PMMA and PEMA materials render them effective adhesion promoters for the surface-segregated fluorodecyl POSS and enhance the mechanical durability of the liquid repellent coatings.

Conclusions

Low surface energy fluorodecyl POSS is a promising material for fabricating liquid repellent coatings,[4,5,19–21,51,58,59,68] but is characterized by a number of drawbacks in its pure form, including high cost, a tendency to deposit from solution as a rough film, a lack of optical transparency, and poor adhesion to underlying substrates. In the present study we have investigated blends comprising 0–50 wt% fluorodecyl POSS dispersed in a Tecnoflon, PMMA, PEMA, or PBMA binder and demonstrated that each of the shortcomings of pure fluorodecyl POSS films can be addressed through dispersion into an appropriately selected polymeric matrix.

The liquid wettability of each blend was probed by measuring advancing and receding contact angles of three polar liquids (water, ethylene glycol, and dimethyl sulfoxide) and three nonpolar fluids (diiodomethane, rapeseed oil, and hexadecane). The resulting contact angle data were concisely represented in the form of wettability diagrams (Fig. 3d and 4d) in which a geometrically-determined drop sliding parameter (eqn (3)) is plotted against a drop pull-off factor (eqn (5)) to intuitively illustrate the relative liquid wettability (or repellency) of each test substrate. Additional quantitative characterization of the test coatings was completed by using the Girifalco-Good framework[43,46–49] to calculate the individual polar, dispersive, and acidic/basic components of advancing and receding surface energy values. While a number of the studied polymer/fluorodecyl POSS coatings were characterized by an advancing surface energy as low as 9 ± 1 mN m^{-1}, the receding solid surface energy values and their individual contributions are sensitive to the specific composition of the polymeric binder. These variations in the energy contributions associated with a receding drop are important because it is low receding interactions that minimize pinning of a receding contact line and the concomitant resistance to both drop sliding (eqn (3)) and drop pull-off (eqn (5)). We emphasize that it is important to consider the individual acidic and basic contributions $\gamma^{+}_{sv,r}$ and $\gamma^{-}_{sv,r}$ because it is the binary solid-liquid interactions $\sqrt{\gamma^{+}_{sv,r}\gamma^{-}_{lv}}$ and $\sqrt{\gamma^{-}_{sv,r}\gamma^{+}_{lv}}$, not the solid polar contribution $\gamma^{p}_{sv,r}$, that influence liquid wettability. Specific acid–base interactions may take place even on surfaces

characterized by very low values of the polar contribution $\gamma^{p}_{sv,r}$ because either: (i) γ^{+}_{lv} or γ^{-}_{lv} is very large; (ii) a near-zero value of $\gamma^{+}_{sv,r}$ (or $\gamma^{-}_{sv,r}$) makes $\gamma^{p}_{sv,r}$ appear negligible even though $\gamma^{-}_{sv,r}$ (or $\gamma^{+}_{sv,r}$) is significant. It is the low values of $\gamma^{d}_{sv,r}$, $\gamma^{+}_{sv,r}$, and $\gamma^{-}_{sv,r}$ that truly distinguish fluorodecyl POSS as a strongly liquid-repellent material.

The weakest solid-liquid interactions were obtained on PMMA/fluorodecyl POSS and PEMA/fluorodecyl POSS blends with fluorodecyl POSS loadings of 20 wt% and above. These PMMA/and PEMA/fluorodecyl POSS materials are characterized by even lower apparent receding surface energy values than pure fluorodecyl POSS coatings, most likely due to the surface roughness of the pure fluorodecyl POSS films. The addition of the PMMA or PEMA matrix phase has a number of other performance benefits besides facilitating the deposition of smooth films. These desirable attributes include reducing the amount of expensive fluorodecyl POSS required to provide maximum liquid repellency, imparting optical transparency to fluorodecyl POSS-based films, and enhancing the adhesion of the liquid repellent coating to underlying substrates. These improvements in performance may facilitate the adoption of fluorodecyl POSS-based materials as coatings in liquid repellency applications.

Acknowledgements

The authors gratefully acknowledge financial support from the Air Force Research Laboratory, Propulsion Directorate, the Air Force Office of Scientific Research, and the Army Research Office through Contract W911NF-07-D-004. A.J.M. acknowledges support from the National Research Council (NRC) for a Postdoctoral Fellowship and A.R.N. thanks the Massachusetts Institute of Technology (MIT) Materials Processing Center and MIT Center for Materials Science and Engineering (CMSE) for support through the NSF REU program. We thank Prof. Michael F. Rubner for the use of the contact angle goniometer, Mr. J. David Smith and Prof. Kripa K. Varanasi for providing the Teflon AF-2400 solution, the CMSE and the Institute for Soldier Nanotechnologies at MIT for the use of various experimental equipment, Ms. Elizabeth L. Shaw for help with the XPS, and Mr. Siddarth Srinivasan for helpful discussions and assistance with the AFM measurements.

References

1 K. Law, H. Zhao and V. Sambhy, US Patent 20110025752, 2011.
2 S. T. Iacono, S. M. Budy, D. W. Smith and J. M. Mabry, *J. Mater. Chem.*, 2010, **20**, 2979–2984.
3 A. Vilcnik, I. Jerman, A. S. Vuk, M. Kozelj, B. Orel, B. Tomsic, B. Simonic and J. Kovac, *Langmuir*, 2009, **25**, 5869–5880.
4 S. S. Chhatre, A. Tuteja, W. Choi, A. Revaux, D. Smith, J. M. Mabry, G. H. McKinley and R. E. Cohen, *Langmuir*, 2009, **25**, 13625–13632.
5 W. Choi, A. Tuteja, S. Chhatre, J. M. Mabry, R. E. Cohen and G. H. McKinley, *Adv. Mater.*, 2009, **21**, 2190–2195.
6 W. Ming, B. Leng, R. Hoefnagels, D. Wu, G. de With and Z. Shao, *Contact Angle, Wettability Adhes.*, 2009, **6**, 191–205.
7 Y. Gao, C. He, Y. Huang and F. Qing, *Polymer*, 2010, **51**, 5997–6004.
8 R. Misra, R. D. Cook and S. E. Morgan, *J. Appl. Polym. Sci.*, 2010, **115**, 2322–2331.
9 R. N. Wenzel, *Ind. Eng. Chem.*, 1936, **28**, 988–994.
10 A. B. D. Cassie and S. Baxter, *Trans. Faraday Soc.*, 1944, **40**, 546–551.
11 R. E. Johnson, Jr. and R. H. Dettre, *Surfactant Sci. Ser.*, 1993, **49**, 1–73.
12 W. A. Zisman, in *Contact Angle, Wettability, and Adhesion*, ed. F. M. Fowkes, Washington, DC, American Chemical Society, 1964, vol. 43.
13 H. W. Fox and W. A. Zisman, *J. Colloid Sci.*, 1950, **5**, 514–531.
14 H. W. Fox and W. A. Zisman, *J. Colloid Sci.*, 1952, **7**, 109–121.
15 M. J. Owen and H. Kobayashi, *Macromol. Symp.*, 1994, **82**, 115–123.
16 S. R. Coulson, I. S. Woodward, J. P. S. Badyal, S. A. Brewer and C. Willis, *Chem. Mater.*, 2000, **12**, 2031–2038.
17 G. Z. Li, L. C. Wang, H. L. Ni and C. U. Pittman, *J. Inorg. Organomet. Polym.*, 2001, **11**, 123–154.
18 S. H. Phillips, T. S. Haddad and S. J. Tomczak, *Curr. Opin. Solid State Mater. Sci.*, 2004, **8**, 21–29.
19 S. T. Iacono, A. Vij, W. Grabow, D. W. Smith, Jr. and J. M. Mabry, *Chem. Commun.*, 2007, 4992–4994.
20 J. M. Mabry, A. Vij, S. T. Iacono and B. D. Viers, *Angew. Chem., Int. Ed.*, 2008, **47**, 4137–4140.
21 S. S. Chhatre, J. O. Guardado, B. M. Moore, T. S. Haddad, J. M. Mabry, G. H. McKinley and R. E. Cohen, *ACS Appl. Mater. Interfaces*, 2010, **2**, 3544–3554.
22 L. C. Gao and T. J. McCarthy, *Langmuir*, 2008, **24**, 9183–9188.
23 L. C. Gao and T. J. McCarthy, *Langmuir*, 2009, **25**, 14105–14115.
24 M. Strobel and C. S. Lyons, *Plasma Processes Polym.*, 2011, **8**, 8–13.
25 C. W. Extrand and A. N. Gent, *J. Colloid Interface Sci.*, 1990, **138**, 431–442.
26 H. Murase, K. Nanishi, H. Kogure, T. Fujibayashi, K. Tamura and N. Haruta, *J. Appl. Polym. Sci.*, 1994, **54**, 2051–2062.
27 C. Della Volpe, S. Siboni and M. Morra, *Langmuir*, 2002, **18**, 1441–1444.
28 L. Feng, Y. A. Zhang, J. M. Xi, Y. Zhu, N. Wang, F. Xia and L. Jiang, *Langmuir*, 2008, **24**, 4114–4119.
29 C. G. Furmidge, *J. Colloid Sci.*, 1962, **17**, 309–324.
30 E. Wolfram and R. Faust, in *Wetting, Spreading, and Adhesion*, London, Academic Press, 1978, pp. 213–222.
31 E. Pierce, F. J. Carmona and A. Amirfazli, *Colloids Surf., A*, 2008, **323**, 73–82.
32 C. Antonini, F. J. Carmona, E. Pierce, M. Marengo and A. Amirfazil, *Langmuir*, 2009, **25**, 6143–6154.
33 W. Choi, A. Tuteja, J. M. Mabry, R. E. Cohen and G. H. McKinley, *J. Colloid Interface Sci.*, 2009, **339**, 208–216.
34 T. Young, *Philos. Trans. R. Soc. London*, 1805, **95**, 65.
35 A. Dupre, *Theorie Mecanique de la Chaleur*, Paris, Gauthier-Villars, 1869.
36 J. C. Berg, *Surfactant Sci. Ser.*, 1993, **49**, 75–148.
37 P. C. Hiemenz and R. Rajagopalan, *Principles of Colloid and Surface Chemistry*, New York, Marcel Dekker, 1997.
38 A. Marmur, *Soft Matter*, 2006, **2**, 12–17.
39 A. Marmur, *Annu. Rev. Mater. Res.*, 2009, **39**, 473–489.
40 E. J. de Souza, L. C. Gao, T. J. McCarthy, E. Arzt and A. J. Crosby, *Langmuir*, 2008, **24**, 1391–1396.
41 K. L. Mittal, in *Adhesion Measurement of Thin Films, Thick Films and Bulk Coatings*, Philadelphia, PA, ASTM Special Tech. Publ. 640, 1976.
42 R. J. Good, N. R. Srivatsa, M. Islam, H. T. L. Huang and C. J. Van Oss, *J. Adhes. Sci. Technol.*, 1990, **4**, 607–617.
43 R. J. Good, *J. Adhes. Sci. Technol.*, 1992, **6**, 1269–1302.
44 C. Della Volpe and S. Siboni, *J. Colloid Interface Sci.*, 1997, **195**, 121–136.
45 D. K. Owens and R. C. Wendt, *J. Appl. Polym. Sci.*, 1969, **13**, 1741–1747.
46 L. A. Girifalco and R. J. Good, *J. Phys. Chem.*, 1957, **61**, 904–909.
47 R. J. Good, *J. Colloid Interface Sci.*, 1977, **59**, 398–419.
48 C. J. Van Oss, R. J. Good and M. K. Chaudhury, *Langmuir*, 1988, **4**, 884–891.
49 C. J. Van Oss, M. K. Chaudhury and R. J. Good, *Chem. Rev.*, 1988, **88**, 927–941.
50 M. K. Chaudhury, *Mater. Sci. Eng., R*, 1996, **16**, 97–159.
51 A. Tuteja, W. Choi, M. Ma, J. M. Mabry, S. A. Mazzella, G. C. Rutledge, G. H. McKinley and R. E. Cohen, *Science*, 2007, **318**, 1618–1622.
52 S. Turri and M. Levi, *Macromol. Rapid Commun.*, 2005, **26**, 1233–1236.
53 R. Misra, B. X. Fu, A. Plagge and S. E. Morgan, *J. Polym. Sci., Part B: Polym. Phys.*, 2009, **47**, 1088–1102.
54 P. F. Rios, H. Dodiuk, S. Kenig, S. McCarthy and A. Dotan, *J. Adhes. Sci. Technol.*, 2006, **20**, 563–587.

55 K. Koh, S. Sugiyama, T. Morinaga, K. Ohno, Y. Tsujii, T. Fukuda, M. Yamahiro, T. Iijima, H. Oikawa, K. Watanabe and T. Miyashita, *Macromolecules*, 2005, **38**, 1264–1270.
56 J. W. Xu, X. Li, C. M. Cho, C. L. Toh, L. Shen, K. Y. Mya, X. H. Lu and C. B. He, *J. Mater. Chem.*, 2009, **19**, 4740–4745.
57 F. Mammeri, C. Bonhomme, F. Ribot, F. Babonneau and S. Dire, *Chem. Mater.*, 2009, **21**, 4163–4171.
58 A. Tuteja, W. Choi, G. H. McKinley, R. E. Cohen and M. F. Rubner, *MRS Bull.*, 2008, **33**, 752–758.
59 A. Tuteja, W. Choi, J. M. Mabry, G. H. McKinley and R. E. Cohen, *Proc. Natl. Acad. Sci. U. S. A.*, 2008, **105**, 18200–18205.
60 L. Z. Dai, C. J. Yang, Y. T. Xu, Y. M. Deng, J. F. Chen, J. Galy and J. F. Gerard, *Sci. China Chem.*, 2010, **53**, 2000–2005.
61 A. J. Meuler, J. D. Smith, K. K. Varanasi, J. M. Mabry, G. H. McKinley and R. E. Cohen, *ACS Appl. Mater. Interfaces*, 2010, **2**, 3100–3110.
62 R. Misra, B. X. Fu and S. E. Morgan, *J. Polym. Sci., Part B: Polym. Phys.*, 2007, **45**, 2441–2455.
63 K. Zeng and S. Zheng, *J. Phys. Chem. B*, 2007, **111**, 13919–13928.
64 J. M. Mabry, A. Vij, B. D. Viers, W. W. Grabow, D. Marchant, S. T. Iacono, P. N. Ruth and I. Vij, in *ACS Symposium Series 964*, ed. S. Clarson, J. J. Fitzgerald, M. J. Owen, S. S. Smith and M. E. Van Dyke, Washington, DC, American Chemical Society, 2007, pp. 290–300.
65 I. Jerman, M. Kozelj and B. Orel, *Sol. Energy Mater. Sol. Cells*, 2010, **94**, 232–245.
66 S. T. Iacono, S. M. Budy, J. M. Mabry and D. W. SmithJr, *Macromolecules*, 2007, **40**, 9517–9522.
67 S. T. Iacono, S. M. Budy, J. M. Mabry and D. W. Smith, Jr., *Polymer*, 2007, **48**, 4637–4645.
68 S. S. Chhatre, W. Choi, A. Tuteja, K.-C. Park, J. M. Mabry, G. H. McKinley and R. E. Cohen, *Langmuir*, 2010, **26**, 4027–4035.
69 S. Lee, J. S. Park and T. R. Lee, *Langmuir*, 2008, **24**, 4817–4826.
70 C. Della Volpe, A. Deimichei and T. Ricco, *J. Adhes. Sci. Technol.*, 1998, **12**, 1141–1180.
71 T. Bialopiotrowicz, *J. Adhes. Sci. Technol.*, 2009, **23**, 799–813.
72 T. Bialopiotrowicz, *J. Adhes. Sci. Technol.*, 2009, **23**, 815–825.
73 R. J. Good and C. J. Van Oss, in *Modern Approaches to Wettability: Theory and Applications*, ed. M. Schrader and G. Loeb, New York, Plenum, 1992, pp. 1–27.
74 ASTM Standard D3359-09, *Test Methods for Measuring Adhesion by Tape Test*, ASTM International, 2010.
75 H. Kamusewitz, W. Possart and D. Paul, *Colloids Surf., A*, 1999, **156**, 271–279.
76 S. Kirk, M. Strobel, C. Lee, S. J. Pachuta, M. Prokosch, H. Lechuga, M. E. Jones, C. S. Lyons, S. Degner, Y. Yang and M. J. Kushner, *Plasma Process. Polym.*, 2010, **7**, 107–122.
77 DuPont, http://www2.dupont.com/Teflon_Industrial/en_US/assets/downloads/h44015.pdf.
78 C. W. Extrand, in *Encyclopedia of Colloid and Surface Science*, ed. P. Somasundaran, Boca Raton, FL, CRC Press, 2006, vol. 4, pp. 2876–2891.
79 Y. Mao and K. K. Gleason, *Macromolecules*, 2006, **39**, 3895–3900.
80 D. L. Schmidt, C. E. Coburn, B. M. Dekoven, G. E. Potter, G. F. Meyers and D. A. Fischer, *Nature*, 1994, **368**, 39–41.
81 D. Y. Kwok and A. W. Neumann, *Adv. Colloid Interface Sci.*, 1999, **81**, 167–249.